## EDGE ARTICLE

Check for updates

# Chiral oxazolidines acting as transient hydroxyalkyl-functionalized N-heterocyclic carbenes: an efficient route to air stable copper and gold complexes for asymmetric catalysis†

Delphine Pichon-Barré, [ID] [a] Ziyun Zhang,[d] Aël Cador,[a] Thomas Vives, [ID] [a] Thierry Roisnel, [ID] [a] Olivier Baslé, [ID] [b] Lucie Jarrige, [ID] [a] Luigi Cavallo, [ID] *[d] Laura Falivene [ID] *[c] and Marc Mauduit [ID] *[a]

Optically pure oxazolidines were synthesized in nearly quantitative yields from chiral hydroxyalkyl-functionalized imidazolinium salts. Acting as transient chiral diamino N-heterocyclic carbenes (NHCs), these oxazolidines allowed the efficient formation of well-defined copper(I) and gold(I) hydroxyalkyl-NHC complexes, which could be isolated, for the first time, as air stable complexes after silica gel chromatography. Interestingly, X-ray analysis of gold complexes revealed that the hydroxyl-function is not chelated to the metal. Computational studies suggested that both cyclisation to produce oxazolidine and O−H bond elimination to form the transient carbene (prior to coordination) occur through a concerted mechanism. The novel chiral copper-catalysts, as well as oxazolidines alone (copper free), demonstrated excellent performances in asymmetric conjugate addition and allylic alkylation with high regio- and enantio-selectivities (up to 99% ee).

## Introduction

Since their discovery in the early 1960s, N-heterocyclic carbenes (NHCs) have become privileged ligands for numerous transition metal (TM) catalysed transformations, in both academic and industrial research environments.[1] Due to their remarkable ability to generate a strong sigma-bond with the metal, these ancillary ligands improved drastically the catalyst activities, even surpassing the popular phosphorus-based ligands. With a versatile and highly modular steric environment, exploration of chiral NHCs as stereo-directing ligands has naturally emerged in the early 1990s. With resounding successes, their use in enantioselective catalysis has greatly accelerated in the last decade. Thanks to their easy and straightforward synthetic access, a plethora of chiral NHC ligands featuring various elements of symmetry were developed and studied in

asymmetric catalysis.[2] Among them, the class of diaminocarbene precursors **L**H·X bearing a chiral hydroxyalkyl-chelating side chain (Fig. 1a), readily accessible in 1 to 5 steps,[3] has proved to be quite efficient in copper-catalysed enantioselective transformations.[4] Notably, fruitful applications were achieved in copper-catalysed Asymmetric Conjugated Addition (ACA) and Asymmetric Allylic Alkylation (AAA), two major organometallic reactions for the formation of C–C bonds.[5]

A wide range of Zn-, Mg-, B- and Al-based organometallic nucleophiles and Michael acceptors or allylic substrates were investigated leading to numerous building-blocks, including challenging chiral all-carbon quaternary centers, in good to excellent yields with remarkable enantioselectivities (up to 99% ee).[6] Moreover, these highly selective catalytic methodologies were successfully applied in the total synthesis of complex natural products.[7] Noteworthy, all catalytic transformations were exclusively done through the *in situ* formation of related Cu-catalytic species by just mixing **L**H·X (X = Cl or PF$_6$), a base[8] and Cu(I)- or Cu(II)-salts. Nevertheless, several DFT studies were accomplished enabling to propose some mechanistic insights to explain the high levels of regio- and enantioselectivity reached, notably in the case of polyconjugated substrates.[9] Unfortunately, all attempts to isolate and characterize a well-defined chiral chelating copper–hydroxyalkyl–NHC complex have failed. In 2008, Arnold and co-workers reported the successful synthesis of chelating alkoxy-NHC yttrium complex

*[a]Univ Rennes, Ecole Nationale Supérieure de Chimie de Rennes, CNRS, ISCR UMR 6226, F-35000 Rennes, France. E-mail: marc.mauduit@ensc-rennes.fr*
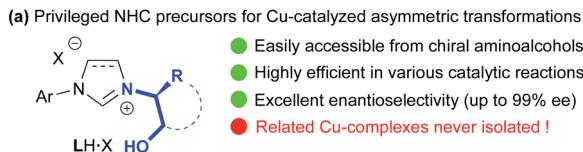
*[b]LCC-CNRS, Université de Toulouse, CNRS, Toulouse, France*

*[c]Dipartimento di Chimica, Università di Salerno, Via Ponte Don Melillo, I-84084 Fisciano, Italy. E-mail: lafalivene@unisa.it*
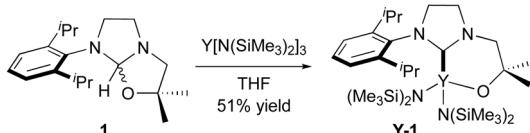
*[d]King Abdullah University of Science and Technology (KAUST), Chemical and Life Sciences and Engineering, Kaust Catalysis Center, Thuwal 23955-6900, Saudi Arabia. E-mail: luigi.cavallo@kaust.edu.sa*

**(a)** Privileged NHC precursors for Cu-catalyzed asymmetric transformations

● Easily accessible from chiral aminoalcohols
● Highly efficient in various catalytic reactions
● Excellent enantioselectivity (up to 99% ee)
● Related Cu-complexes never isolated !

**LH·X**

**(b)** Arnold *et al.* (2008):

Y[N(SiMe₃)₂]₃
THF
51% yield

**1**

**Y-1**

**(c)** Oxazolidines as transient chiral NHCs (**this work**):

KHMDS
quantitative

**L1H·Cl**

Air-stable oxazolidine **2**

Excellent catalytic performances in copper free-AAA (up to **96% ee**)

Ar = 2,6-$^i$Pr-C₆H₃ (DIPP) or 2,4,6-Me-C₆H₂ (Mes)

**MX·SMe₂**

MX = AuCl or CuBr

Air-stable chiral complexes

Excellent catalytic performances in Cu-AAA & Cu-ACA (up to **>99% ee**)
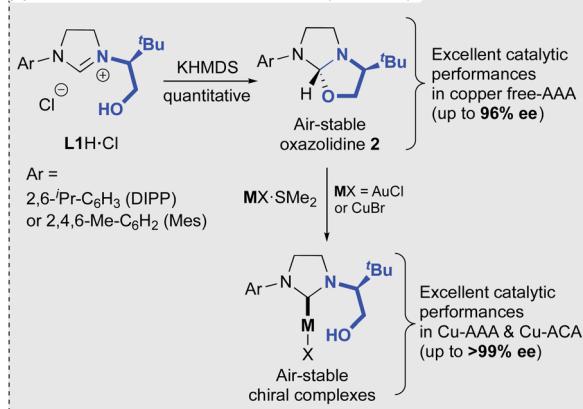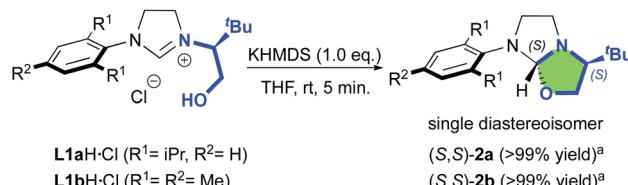
**Fig. 1** (a) Privileged chelating hydroxyalkyl–NHC ligand precursors for Cu-catalysed asymmetric transformations. (b) Previous synthesis of hydroxyl-chelating NHC–yttrium complex from achiral oxazolidine. (c) Proposed synthetic route to chiral hydroxyalkyl-functionalized NHC copper and gold complexes (this work).

**Y-1** (Fig. 1b) from achiral oxazolidine **1**, suggesting the formation of a transient carbene.[10] We report herein that chiral hydroxyalkyl–NHC copper and gold complexes may be readily formed from oxazolidine intermediate **2** derived from optically pure imidazolinium salts **L1**H·Cl (Fig. 1c). The solid-state structure of gold complexes show that hydroxyl-function is not coordinated to the metal. The mechanisms for both the oxazolidine and the transient carbene formation as well as the metal insertion are supported by DFT calculations. Additionally, the resulting well-defined chiral copper-catalysts, as well as the oxazolidines, demonstrate excellent catalytic performances in Cu-AAA and Cu-ACA.

## Results and discussion

Our study began with the preparation of oxazolidines **2** from the well-known hydroxyalkyl-imidazolinium chloride salts **L1a**H·Cl and **L1b**H·Cl featuring either a N-2,6-diisopropylphenyl (DIPP) or a N-2,4,6-trimethylphenyl (Mes) substituent in association with a N-(S)*tert*-leucinol moiety (Scheme 1).[3a] After a rapid screening of several bases (see ESI† for details), potassium hexamethyldisilazide (KHMDS) appeared the most effective one producing exclusively oxazolidines **2a** and **2b** within 5 minutes at ambient temperature. These latter were then isolated in quantitative yields after a simple filtration through a pad of

KHMDS (1.0 eq.)
THF, rt, 5 min.

single diastereoisomer

**L1a**H·Cl (R¹= iPr, R²= H)
**L1b**H·Cl (R¹= R²= Me)

(S,S)-**2a** (>99% yield)[a]
(S,S)-**2b** (>99% yield)[a]

**Scheme 1** KHMDS-mediated diastereoselective formation of oxazolidines **2a,b**. [a]Isolated yield after silica gel filtration.
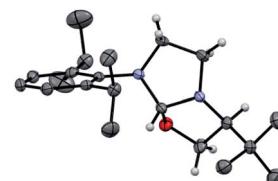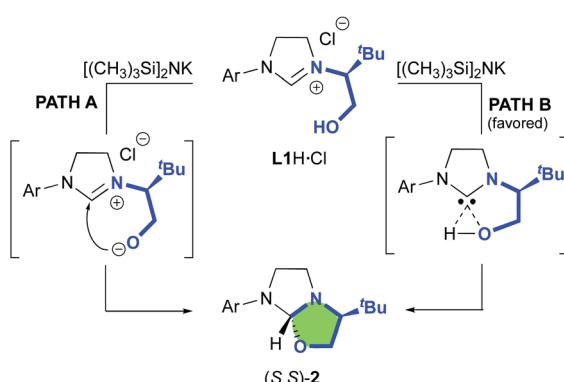
**Fig. 2** Solid-state structure of oxazolidine (S,S)-**2a** from single crystal X-ray diffraction. Displacement ellipsoids are drawn at 50% probability. Most hydrogen atoms have been omitted for clarity (N in purple, C in grey, O in red, H in white).

Celite. Interestingly, similar high yields were also obtained at 500 mg scale (see ESI† for details). In accordance with Marazano works,[11] the cyclisation occurred in opposite way to the *tert*-butyl group leading to a *trans* relationship between the two stereogenic carbons. This structural feature was confirmed by X-ray diffraction analysis of oxazolidine **2a**, allowing to attribute the absolute configuration of the new stereogenic center (S, Fig. 2). As two possible pathways could be envisaged involving either the deprotonation of the hydroxyl function followed by the nucleophile addition of the resulting alcoholate to the iminium (path A, Scheme 2)[12] or the deprotonation of imidazolinium proton and the subsequent carbene insertion to the OH bond (path B), mechanistic insights were investigated by DFT calculations (Fig. 3).[13]

Starting from **L1a**H, set as zero-point energy, both deprotonated species are energetically favored, with the carbene intermediate **C** being 31.2 kcal mol⁻¹ more stable than **L1a**H and the alternative alcoholate lying at −16 kcal mol⁻¹, *i.e.*

**PATH A**
[(CH₃)₃Si]₂NK

**PATH B** (favored)
[(CH₃)₃Si]₂NK

**L1H·Cl**

(S,S)-**2**

**Scheme 2** Plausible pathways for cyclisation leading to oxazolidine (S,S)-**2**.
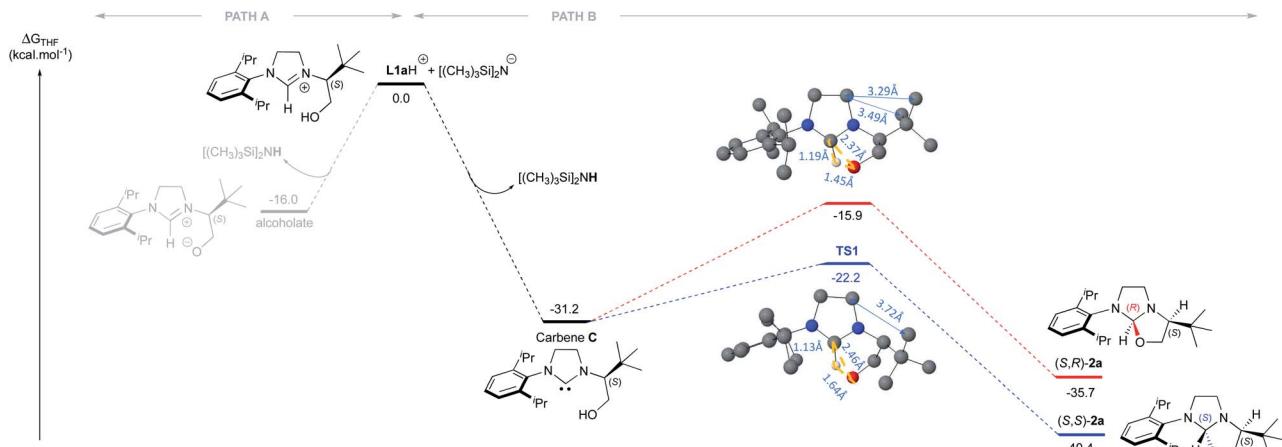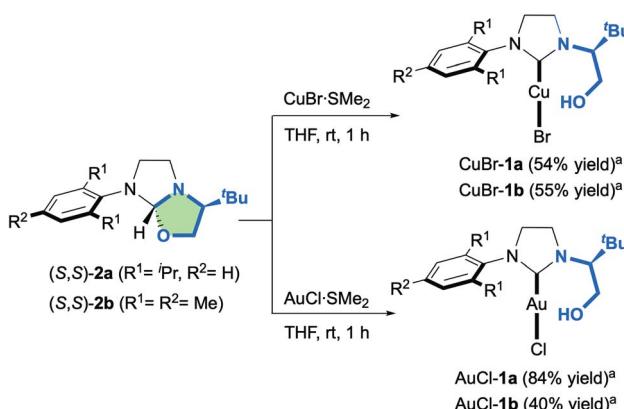
**Fig. 3** DFT calculations regarding the mechanism of the oxazolidine $(S,S)$-**2a** formation from **L1a**H. (The Cl$^-$ and K$^+$ were not considered in the calculations).

15.2 kcal mol$^{-1}$ higher in energy with respect to carbene **C** (Fig. 3). Starting from the thermodynamically favored carbene species **C**, the formation of the C–O bond and the transfer of the proton from oxygen to carbon are synchronous and lead directly to the formation of oxazolidine **2a** in a concerted event. Any attempts to localize a stepwise mechanism failed. The reductive elimination transition state **TS1** requires an energy barrier relative to **C** of 9.1 and 15.3 kcal mol$^{-1}$ for the formation of $S,S$ and $S,R$ product, respectively. The resulting oxazolidine $(S,S)$-**2a** at $-40.4$ kcal mol$^{-1}$ is thermodynamically more favored by almost 5 kcal mol$^{-1}$ respect to $(S,R)$-**2a** lying at $-35.7$ kcal mol$^{-1}$. The calculated $\Delta\Delta G^{\neq}$ of 6.3 kcal mol$^{-1}$ between the two enantiomeric transitions states clearly indicates the exclusive formation of the $(S,S)$-**2a** product, in agreement with experiments. The analysis of transition state geometries highlights that the unfavored $(S,R)$-**TS1** is destabilized by steric repulsions between the NHC backbone and the *tert*-butyl group (see short distances in Fig. 3).

Having these optically pure oxazolidine $(S,S)$-**2a,b** in hand, the introduction of transition metals to yield corresponding chelating hydroxyalkyl–NHC–metal complexes was next investigated (Scheme 3). While **2a,b** remained totally inert toward CuCl salt, we were delighted to observe that CuBr·SMe$_2$ enabled the formation of novel air-stable copper complexes CuBr-**1a** and CuBr-**1b** in respectively 54% and 55% yields after silica gel purification.

Similarly, the reaction with AuCl·SMe$_2$ produced the NHC-gold complexes AuCl-**1a** and AuCl-**1b** in 84% and 40% isolated yields after purification. Interestingly, the $^1$H-NMR analysis showed that the hydroxyl-functionality was not chelated to the metal. This structural feature was unambiguously confirmed by solid-state structure analysis of AuCl-**1a,b** complexes by X-ray diffraction (Fig. 4). Intrigued by the presence of the free hydroxyl function, DFT calculations about the transient carbene formation and the gold-metal insertion were next investigated (Fig. 5). Starting from oxazolidine $(S,S)$-**2a**, the backward reductive elimination transition state **TS1** requires an energy barrier of 18.3 kcal mol$^{-1}$ with the transient carbene **C** being almost 9 kcal mol$^{-1}$ higher than the reactant. However, the following gold insertion step occurs easily with a relatively low energy barrier of only 5.4 kcal mol$^{-1}$ with respect to carbene **C**, pushing the reaction towards the product. Overall, the thermochemistry of the reaction is estimated to be highly exergonic, with AuCl-**1a** complex plus SMe$_2$ being at $-21.4$ kcal mol$^{-1}$



**Scheme 3** Synthesis of chiral hydroxyalkyl–NHC CuBr-**1a,b** and AuCl-**1a,b** complexes from oxazolidines **2a,b**. $^a$Isolated yields after silica gel filtration.
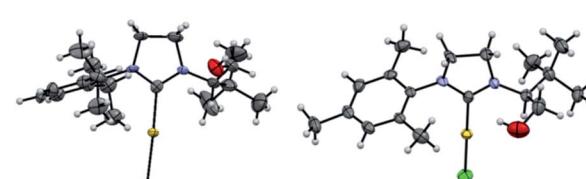


**Fig. 4** Solid-state structure of AuCl-**1a** (left) and AuCl-**1b** (right) complexes from single crystal X-ray diffraction. Displacement ellipsoids are drawn at 50% probability. Most hydrogen atoms have been omitted for clarity (N in purple, C in grey, O in red, H in white, Cl in green and Au in yellow). For AuCl-**1b**, only one molecule of the asymmetric unit is shown (see ESI† for details).
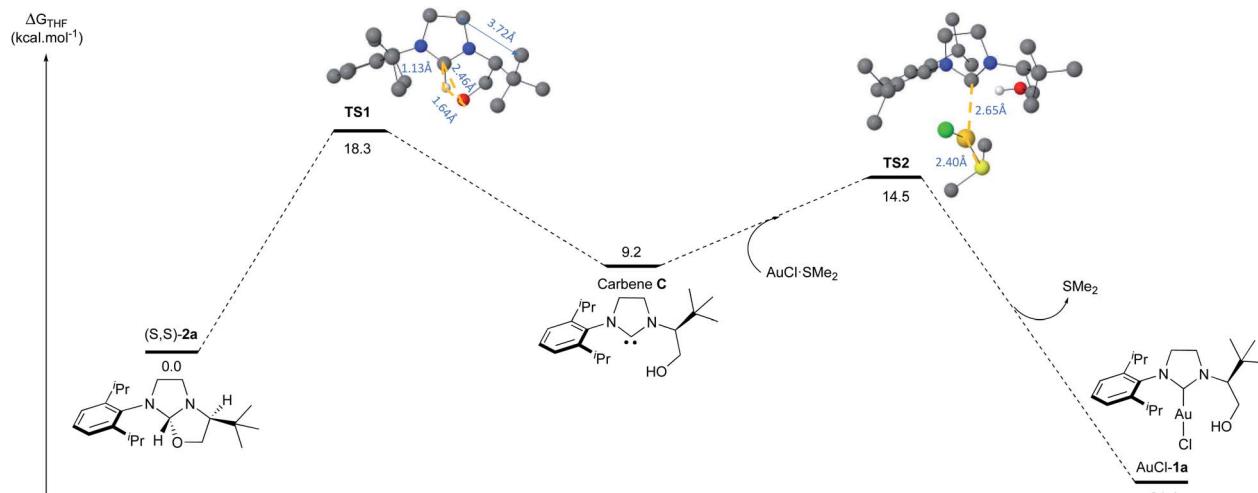
**Fig. 5** DFT calculations regarding the mechanism of the transient carbene formation from oxazolidine (S,S)-**2a** followed by the gold insertion to produce AuCl-**1a** complex.
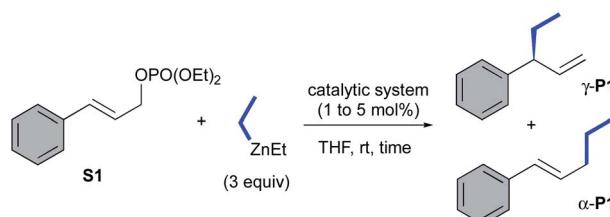
respect to (S,S)-**2a** plus AuCl·SMe$_2$. Any attempts to localize transition states for coordination of gold to the carbene carbon before oxygen leaves were ruled out due to the higher energy barriers involved.

The catalytic performances of these new transient carbene precursors (S,S)-**2a,b** and their related copper catalysts CuBr-**1a,b** were further evaluated in asymmetric catalysis. The allylic alkylation of cinnamyl phosphate **S1** with diethylzinc was first studied (Table 1). In comparison with the previously reported catalytic system **L1aH·PF$_6$/(CuOTf)$_2$·toluene** which required the prior deprotonation of the imidazolinium salt by n-BuLi to form

the corresponding Cu–NHC catalytic species,[6a,14] we were delighted to observe a similar catalytic performance with oxazolidine **2a** in presence of (CuOTf)$_2$·toluene complex (entries 1 and 2). A full-conversion occurred within 30 minutes at ambient temperature with the exclusive formation of the expected product γ-**P1** in 92% isolated yield and 89% ee. With CuBr·SMe$_2$, oxazolidine (S,S)-**2a** led also to γ-**P1** in a slightly higher 97% yield and 88% ee (entry 3).

As expected, the well-defined and air stable copper catalyst CuBr-**1a** (1 mol%) gave similar high efficiency affording γ-**P1** in quantitative yield and 89% ee (entry 4). Interestingly, without

**Table 1** Evaluation of oxazolidines **2a,b** and CuBr-**1a,b** in AAA of cinnamyl phosphate **S1**



| Entry | Catalytic system (mol%) | Time (h) | Conv.[a] (yield)[b] (%) | γ/α-**P1** ratio[c] | ee[d] (%) |
|---|---|---|---|---|---|
| 1[e] | **L1aH·PF$_6$/(CuOTf)$_2$·tol** (1.2/1) | 0.5 | >99 (62) | >99 : 1 | 90 |
| 2 | **2a/(CuOTf)$_2$·tol** (1.2/1) | 0.5 | >99 (92) | >99 : 1 | 89 |
| 3 | **2a/CuBr·SMe$_2$** (1.2/1) | 0.5 | >99 (97) | >99 : 1 | 88 |
| 4 | **CuBr-1a** (1) | 0.5 | **>99 (99)** | **>99 : 1** | **89** |
| 5 | **2a** (5) | 12 | **>99 (98)** | **>99 : 1** | **90** |
| 6 | **2a** (1) | 23 | 87 (76)[f] | 97 : 3 | 91 |
| 7 | **CuBr-1b** (1) | 0.5 | >99 (88) | >99 : 1 | 87 |
| 8 | **2b** (5) | 12 | Nr | Nd | Nd |
| 9 | **CuBr-1a** (1) with EtMgBr | 0.5 | **>99 (92)** | **>99 : 1** | **90** |
| 10 | **2a** (5) with EtMgBr | 0.5 | >99 (Nd) | 21 : 79 | 39 |

[a] Conversions were monitored by TLC. [b] Isolated yields of γ-**P1** after silica gel chromatography. [c] Molar ratio of γ/α adduct were monitored by $^1$H NMR spectroscopy analysis of the crude mixture. [d] Enantiomeric excesses were determined by chiral-phase GC analysis. [e] Reaction conditions: **L1aH·PF$_6$** (1.2 mol%), n-BuLi (2.5 mol%), (CuOTf)$_2$·tol (0.5 mol%), THF, 0 °C, Et$_2$Zn (3 equiv.), then **S1**, rt. [f] Conversion and yield were determined by $^1$H NMR spectroscopy (see ESI for details). Nr = no reaction. Nd = not determined.

© 2022 The Author(s). Published by the Royal Society of Chemistry
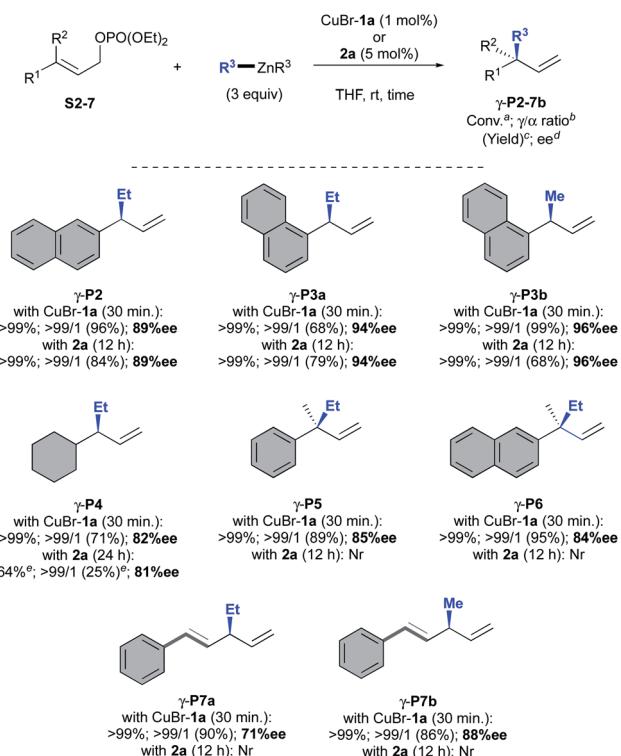
copper,[15] **2a** was also able to catalyse efficiently the addition of Et$_2$Zn, producing the desired γ-**P1** in excellent 98% yield with the same performance of chiral induction (90% ee, entry 5).[16,17] Remarkably, **2a** remained active as low as 1 mol% affording the ramified product γ-**P1** in respectable 76% yield and up to 91% ee (entry 6); nevertheless, a prolonged reaction time (23 h) were required. Changing from Dipp to Mes *N*-substituent did not influence dramatically the reaction as CuBr-**1b** complex gave similar results in terms of chiral induction as well as reactivity (entries 4 and 7). However, the chiral oxazolidine (*S*,*S*)-**2b** surprisingly remained inert, as no conversion was observed (entry 8 *vs*. entry 5). It is worth mentioning that Grignard reagent (EtMgBr) also provided similar excellent results when CuBr-**1a** was employed as catalytic system affording expected product γ-**P1** with 90% ee and 92% isolated yield (entry 9). In contrast, a dramatic drop of selectivity was observed in copper-free conditions with **2a**, leading to a mixture of non-separable regioisomers γ- : α-**P1** in a 21 : 79 ratio (entry 10). Of note, AuCl-**1a,b** complexes were inactive in AAA.[18]

Next, the scope of the AAA was explored with both CuBr-**1a** and oxazolidine **2a** as catalytic systems across a broad range of allylic phosphates and dialkylzinc reagents (Scheme 4). As previously observed, the same excellent levels of efficiency, regio- and stereoselectivity were obtained with or without
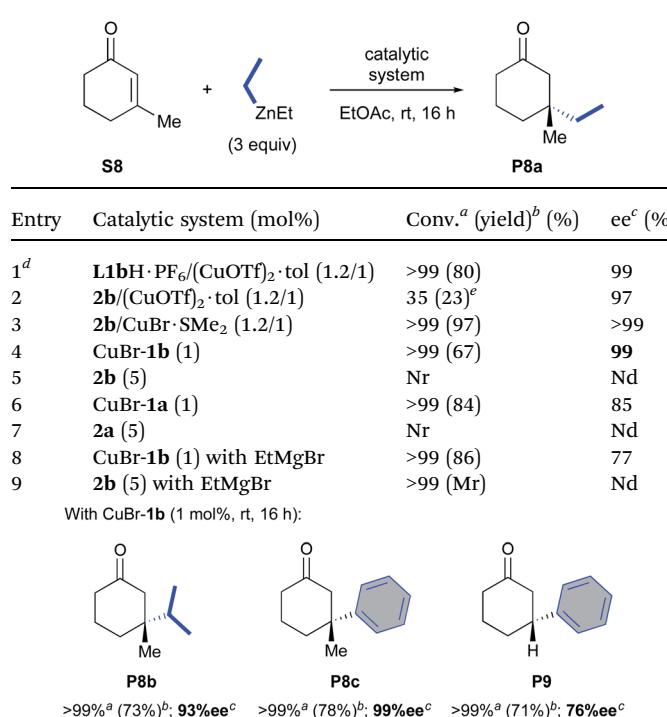
copper for 2-naphthyl and 1-naphthyl-substituted substrates **S2** and **S3** giving corresponding γ-adducts **P2** and **P3a** in 89 and 94% ees, respectively. Interestingly, the methodology was successfully extended to dimethylzinc reagent that led to expected methylated compound γ-**P3b** in good to excellent yields and very high enantioselectivities (96% ee *vs*. 94% ee with Et$_2$Zn).

In the case of the cyclohexyl-derived substrate **S4**, however, the copper-free catalytic system showed less efficiency than CuBr-**1a** as a significant drop of conversion was observed for γ-**P4** (64 *vs*. 99%) but similar good enantiomeric excesses were obtained (81 and 82% ee, respectively). Unfortunately, oxazolidine **2a** alone was unable to promote the formation of chiral all-carbon quaternary centers from trisubstituted allylic phosphate **S5–6**. On the other hand, well-defined CuBr-**1a** complex furnished the desired products γ-**P5** and γ-**P6** with good to excellent isolated yields (89 and 95%, respectively) and satisfactory enantioselectivities (85 and 84% ee). To our delight, a remarkable full γ-selectivity was also observed when diethyl- or dimethylzinc were reacted to the more challenging dienic conjugate substrate **S7** in the presence of CuBr-**1a**. Highly desirable 1,3-skipped dienes γ-**P7a** and γ-**P7b** were thus isolated in 90–86% yield with good to excellent enantioselectivity (71 and 88% ee,

**Scheme 4** Scope of AAA catalysed by oxazolidine **2a** and CuBr-**1a**. [a]Conversions were monitored by TLC. [b]Molar ratio of γ/α adduct were monitored by ^{1}H NMR spectroscopy analysis on the crude mixture. [c]Isolated yields after silica gel chromatography. [d]ee were determined by chiral-phase GC or HPLC analysis. [e]Conversion and yield were determined by ^{1}H NMR spectroscopy (see ESI† for details). Nr = no reaction.

**Table 2** Evaluation of oxazolidines **2a,b** and CuBr-**1a,b** in ACA of cyclic enones

| Entry | Catalytic system (mol%) | Conv.[a] (yield)[b] (%) | ee[c] (%) |
|---|---|---|---|
| 1[d] | **L1bH·PF$_6$**/(CuOTf)$_2$·tol (1.2/1) | >99 (80) | 99 |
| 2 | **2b**/(CuOTf)$_2$·tol (1.2/1) | 35 (23)[e] | 97 |
| 3 | **2b**/CuBr·SMe$_2$ (1.2/1) | >99 (97) | >99 |
| 4 | CuBr-**1b** (1) | >99 (67) | **99** |
| 5 | **2b** (5) | Nr | Nd |
| 6 | CuBr-**1a** (1) | >99 (84) | 85 |
| 7 | **2a** (5) | Nr | Nd |
| 8 | CuBr-**1b** (1) with EtMgBr | >99 (86) | 77 |
| 9 | **2b** (5) with EtMgBr | >99 (Mr) | Nd |

With CuBr-**1b** (1 mol%, rt, 16 h):

**P8b**
>99%[a] (73%)[b]; **93%ee**[c]

**P8c**
>99%[a] (78%)[b]; **99%ee**[c]

**P9**
>99%[a] (71%)[b]; **76%ee**[c]

[a] Conversions were monitored by TLC. [b] Isolated yields after silica gel chromatography. [c] Enantiomeric excesses were determined by chiral-phase GC analysis. [d] Reaction conditions: **L1bH·PF$_6$** (1.2 mol%), *n*-BuLi (2.5 mol%), (CuOTf)$_2$·tol (0.5 mol%), THF, 0 °C, Et$_2$Zn, then **S8**, rt. [e] Conversion and yield were determined by ^{1}H NMR spectroscopy (see ESI for details). Nr = no reaction. Nd = not determined. Mr = Messy reaction.

respectively). Nevertheless, oxazolidine **2a** remained unreactive toward **S7** without cooper salts.
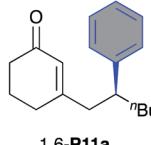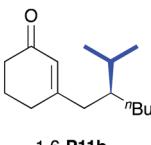
The good catalytic performances demonstrated in AAA prompted us to further evaluate oxazolidines **2a,b** and copper-catalysts CuBr-**1a,b** in ACA of diethylzinc to 3-methylcyclohex-2-enone **S8** (Table 2). Surprisingly, although an excellent 97% ee was obtained for 1,4-product **P8a**, the combination of oxazolidine **2b** with $(CuOTf)_2 \cdot tol$ appeared significantly less productive (35% conv., 23% yield, entry 2) than the *in situ* catalytic system involving the NHC precursor **L1b**H·PF$_6$ and $(CuOTf)_2 \cdot tol$ (>99% conv., 80% yield, entry 1). On the other hand, when **2b** was used in presence of CuBr·SMe$_2$, an excellent 97% isolated yield was obtained in combination with a full enantioselectivity (>99% ee, entry 3). To our delight, air stable CuBr-**1b** gave also a good catalytic performance while unfortunately, oxazolidine **2b** appeared totally inactive without copper salts (entries 4 and 5). Similar behaviours were observed with oxazolidine **2a** and CuBr-**1a** featuring a DIPP N-moiety (entries 6 and 7). The latter afforded **P8a** in good 84% isolated yield despite a slight drop of selectivity (85% ee, entry 6). Ethyl-magnesium bromide was also evaluated in the ACA reaction. Once again, the desired compound **P8a** was exclusively formed when CuBr-**1b** complex was used as catalyst, with a good 86% yield despite a lower enantioselectivity (77% ee). Additionally, although a complete conversion of the substrate was observed during the reaction catalysed by the oxazolidine **2b**, no trace of the expected compound **P8a** were detected in the messy crude

mixture. Finally, as aforementioned above, AuCl-**1a,b** were also inefficient to catalyse the ACA reaction.

We next investigated the catalytic performances of the CuBr-**1b** complex regarding the ACA of diisopropyl- and diphenyl-zinc to 3-methylcyclohex-2-enone **S8** and cyclohex-2-enone **S9**. Both of conjugate additions implying substrate **S8** delivered the desired products **P8b** and **P8c** with good isolated yields (73 and 78%, respectively) and excellent 93–99% enantioselectivities. It is worth noting that in the case of the less hindered cyclohex-2-enone **S9**, a notable drop of the stereoselectivity occurred (76% ee) although the desired compound **P9** was isolated with a satisfying 71% yield.
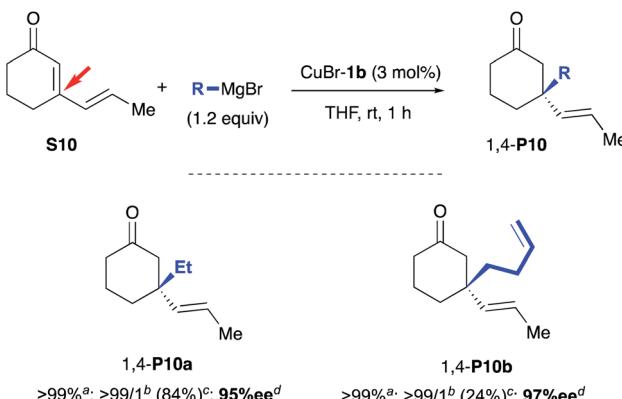
The more challenging 1,6-selective Cu-catalysed ACA of organozincs to cyclic dienone **S10** was then investigated (Table 3). Curiously, the *in situ* catalytic system involving the NHC precursor **L1b**·PF$_6$ and Cu(OTf)$_2$ led only to a messy reaction with no detection of the expected 1,6-product **P10a** (entry 1). With oxazolidine (*S,S*)-**2b** either in combination with Cu(OTf)$_2$ or CuBr·SMe$_2$, 1,6-**P10a** was detected but embedded in a large amount of side products which rendered its isolation unsuccessful (entries 2 and 3). Nevertheless, moderate enantiomeric excesses of respectively 53 and 74% were observed. Advantageously, the use of the well-defined CuBr-**1b** complex allowed us to isolate 1,6-**P10a** in a satisfying 68% yield and a higher enantioselectivity (85% ee, entry 4). Moreover, albeit CuBr-**1a** bearing a bulkier N-DIPP substituent demonstrated a better catalytic performance as the expected 1,6-product was isolated in excellent

**Table 3** Evaluation of oxazolidines **2a,b** and CuBr-**1a,b** in 1,6-ACA of cyclic dienones



| Entry | Catalytic system (mol%) | Conv.[a] (yield)[b] (%) | Selectivity[c] 1,6 : 1,4 | ee[d] (%) |
|---|---|---|---|---|
| 1[e] | **L1b**H·PF$_6$/Cu(OTf)$_2$ (3/2) | Mr | Nd | Nd |
| 2 | **2b**/Cu(OTf)$_2$ (3/2) | >99 (Nd)[f] | >99 : 1 | 53 |
| 3 | **2b**/CuBr·SMe$_2$ (3/2) | >99 (Nd)[f] | >99 : 1 | 74 |
| 4 | CuBr-**1b** (2) | **>99 (68)** | **>99 : 1** | **85** |
| 5 | CuBr-**1a** (2) | > 99 (90) | >99 : 1 | 65 |
| 6 | **2b** (5) | Nr | Nd | Nd |
| 7 | **2a** (5) | Nr | Nd | Nd |

With CuBr-**1b** (2 mol%, same above):



1,6-**P11a**
>99%[a]; >99/1[c] (70%)[b]; **90%ee**[d]

1,6-**P11b**
>99%[a]; >99/1[c] (74%)[b]; **66%ee**[d]

[a] Conversions were monitored by TLC. [b] Isolated yields after silica gel chromatography. [c] Ratios between 1,6 : 1,4-adducts were determined by ^{1}H NMR spectroscopy. [d] Enantiomeric excesses were determined by chiral-phase GC or HPLC analysis. [e] Reaction conditions: (1) **L1b**H·PF$_6$ (3 mol%), n-BuLi (8 mol%), Cu(OTf)$_2$ (2 mol%), THF, 0 °C, Et$_2$Zn, then **S10**, rt. (2) DBU (1 equiv.), CH$_2$Cl$_2$, rt, 5 h. [f] Large amount of side products were formed. Mr = Messy reaction. Nd = not determined. Nr = no reaction.

Scheme 5  1,4-ACA of Grignard reagents to cyclic dienone S10 catalysed by CuBr-**1b** complex. [a]Conversions were monitored by TLC. [b]Ratios between 1,4 : 1,6-adducts were determined by $^1$H NMR spectroscopy analysis on the crude mixture. [c]Isolated yields after silica gel chromatography. [d]ee were determined by chiral-phase GC analysis.

90% yield, a severe drop of the chiral induction was observed (65% ee, entry 5). Of note, by analogy with the aforementioned results in Table 2, oxazolidines **2a,b** were also inefficient under copper-free conditions as no reaction occurred in either cases (entries 6 and 7). Different organozinc reagents were next engaged in this 1,6-ACA reaction with *n*-butyl-chain substituted cyclic dienone **S11**. First, addition of the diphenyl zinc furnished the expected product **P11a** in a regiospecific way with a good 70% isolated yield and an excellent enantioselectivity (90% ee). However, the chiral induction was affected by the use of diisopropylzinc since the corresponding desired compound **P11b** was isolated in 74% yield as a single regioisomer with only 66% ee.

Finally, we directed our attention to Grignard reagents, which led to a complete inversion of the regioselectivity of the conjugate addition[6d,f] in the presence of the CuBr-**1b** complex as catalyst (Scheme 5). Indeed, the exclusive formation of the 1,4 regioisomer was observed and the resulting product 1,4-**P10a** was isolated in a good 84% yield and an excellent 95% ee. Noteworthy, in comparison to the *in situ* catalytic system that required a high catalyst loading (up to 6 mol% of Cu(OTf)$_2$ and 9 mol% of NHC precursor **L1b**H·Cl),[6d,f] a drastic improvement of reactivity was reached here, thanks to use of a well-defined copper complex, as only 3 mol% of CuBr-**1b** was necessary to complete the addition. At last, the 1,4-regiospecificity of the reaction was also confirmed with but-3-en-1-ylmagnesium bromide as nucleophile leading to desired compound 1,4-**P10b** in a similar high enantioselectivity (97%) despite a lower 24% isolated yield.

## Conclusions

In conclusion, well-defined copper(I) and gold(I) complexes containing chiral hydroxyalkyl-functionalized diamino N-heterocyclic carbenes were synthesized for the first time. The strategy involved the formation of optically pure oxazolidines (S,S)-**2a,b**, isolated in quantitative yield from chiral hydroxyalkyl-imidazolinium salts **L1a,b**H·Cl with a complete diastereoselectivity. Advantageously, in the presence of Cu(I)

and Au(I) salts, these oxazolidines were converted to corresponding air-stable CuBr- and AuCl–NHC complexes in good isolated yields. Interestingly, the solid-state structures of the gold-complexes showed that hydroxyl-function is not coordinated to the metal. Computational studies suggested that formation of the oxazolidine operates by concerted O–H bond insertion and that the transient carbene is formed prior to coordination trough concerted O–H bond elimination. Furthermore, resulting copper-catalysts CuBr-**1a,b** afforded excellent catalytic performances in both asymmetric allylic alkylation and 1,6- or 1,4-conjugate addition involving organozinc or Grignard reagents. Excellent regioselectivities were obtained in association with high chiral inductions (up to 99% ee). Noteworthy, air-stable oxazolidines (S,S)-**2a,b** have also demonstrated similar catalytic performances in copper-free AAA transformations. These results will pave the way for the development of more sophisticated hydroxyalkyl-NHC catalytic systems (with or without transition metals[19]) and could offer new opportunities for the discovery of new catalytic reactions.

## Data availability

All experimental and computational data associated with this work are available in the ESI.†

## Author contributions

M. M. conceived, designed and directed the project. D. P.-B. and L. J. conducted all the experiments. A. C., Z. Z., L. F. and L. C. performed the DFT calculations. T. V. developed GC analysis methods while T. R. accomplished of X-ray diffraction analysis. The manuscript was written and reviewed by L. J., O. B., L. C., L. F. and M. M. The ESI† was written by D. P.-B. and L. J.

## Conflicts of interest

There are no conflicts to declare.

## Acknowledgements

## Notes and references

1 (*a*) For a recent book on NHCs, see: S. Díez-González, *N-Heterocyclic Carbenes: From Laboratory Curiosities to*

*Efficient Synthetic Tools*, Royal Society of Chemistry, Cambridge, 2011; (b) M. N. Hopkinson, C. Richter, M. Schedler and F. Glorius, *Nature*, 2014, **510**, 485. For a review dealing with NHC/TM in catalysis, see: (c) S. D. Gonzalez, N. Marion and S. P. Nolan, *Chem. Rev.*, 2009, **109**, 3612; (d) E. Peris, *Chem. Rev.*, 2018, **118**, 9988.

2 For recent reviews on chiral NHCs in catalysis, see:(a) F. Wang, L.-J. Liu, W. Wang, S. Li and M. Shi, *Coord. Chem. Rev.*, 2012, **256**, 804; (b) D. Janssen-Müller, C. Schlepphorst and F. Glorius, *Chem. Soc. Rev.*, 2017, **46**, 4845; (c) J. Thongpaen, R. Manguin and O. Baslé, *Angew. Chem., Int. Ed.*, 2020, **59**, 10242.

3 (a) H. Clavier, L. Coutable, J.-C. Guillemin and M. Mauduit, *Tetrahedron: Asymmetry*, 2005, **16**, 921; (b) H. Clavier, L. Coutable, J.-C. Guillemin and M. Mauduit, *J. Organomet. Chem.*, 2005, **690**, 5237; (c) D. Rix, S. Labat, L. Toupet, C. Crévisy and M. Mauduit, *Eur. J. Inorg. Chem.*, 2009, 1989. For the one-step synthetic route, see: (d) C. Jahier-Diallo, M. S. T. Morin, P. Queval, M. Rouen, I. Artur, P. Querard, L. Toupet, C. Crévisy, O. Baslé and M. Mauduit, *Chem.–Eur. J.*, 2015, **21**, 993; (e) J. Wang, X. Cheng, Y. Liu and J. Zhang, *J. Org. Chem.*, 2021, **86**, 6278.

4 For a review dealing with chiral hydroxyalkyl-NHCs in Copper catalysed-ACA, see: J. Wencel, H. Hénon, S. Kehrli, A. Alexakis and M. Mauduit, *Aldrichimica Acta*, 2009, **42**, 43.

5 For a book chapter or review dealing with metal catalysed-ACA, see:(a) M. Mauduit, O. Baslé, H. Clavier, C. Crévisy and A. Denicourt-Nowicki, in *Comprehensive Organic Synthesis II*, ed. P. Knochel and G. A. Molander, Elsevier, Amsterdam, second edn, 2014, vol. 4, pp. 186–341; (b) C. Hawner and A. Alexakis, *Chem. Commun.*, 2010, **46**, 7295; (c) D. Vargova, I. Nemethova and R. Sebesta, *Org. Biomol. Chem.*, 2020, **18**, 3780. For a book chapter or reviews dealing with Cu-AAA, see: (d) O. Baslé, A. Denicourt-Nowicki, C. Crévisy and M. Mauduit, in *Copper-Catalysed Asymmetric Synthesis*, ed. A. Alexakis, N. Krause and S. Woodward, Wiley-VCH, Weinheim, 2014, chapter 4, pp. 85–126; (e) A. Alexakis, J. E. Backvall, N. Krause, O. Pamies and M. Dieguez, *Chem. Rev.*, 2008, **108**, 2796; (f) S. R. Harutyunyan, T. den Hartog, K. Geurts, A. J. Minnard and B. L. Feringa, *Chem. Rev.*, 2008, **108**, 2824.

6 For selected examples with diorganozinc reagents, see:(a) T. Jennequin, J. Wencel-Delord, D. Rix, J. Daubignard, C. Crévisy and M. Mauduit, *Synlett*, 2010, **11**, 1661; (b) S. Drissi-Amraoui, M. Morin, C. Crévisy, O. Baslé, R. Marcia de Figueiredo, M. Mauduit and J.-M. Campagne, *Angew. Chem., Int. Ed.*, 2015, **54**, 11830. For selected examples with Grignard reagents, see: (c) D. Martin, S. Kehli, M. d'Augustin, H. Clavier, M. Mauduit and A. Alexakis, *J. Am. Chem. Soc.*, 2006, **128**, 8416; (d) H. Henon, M. Mauduit and A. Alexakis, *Angew. Chem., Int. Ed.*, 2008, **47**, 9122; (e) N. Germain, M. Magrez, S. Kehrli, M. Mauduit and A. Alexakis, *Eur. J. Org. Chem.*, 2012, 5301; (f) M. Tissot, D. Poggiali, H. Hénon, D. Müller, L. Guénée, M. Mauduit and A. Alexakis, *Chem.–Eur. J.*, 2012, **18**, 8731; (g) M. Magrez, Y. Le Guen, O. Baslé, C. Crévisy and M. Mauduit, *Chem.–Eur. J.*, 2013, **19**, 1199. For selected

examples with boron nucleophiles, see: (h) R. Shintani, K. Takatsu, M. Takeda and T. Hayashi, *Angew. Chem., Int. Ed.*, 2011, **50**, 8656; (i) F. Meng, X. Li, S. Torker, Y. Shi, X. Shen and A. H. Hoveyda, *Nature*, 2016, **537**, 387; (j) C.-Y. Shi, Z.-Z. Pan, P. Tian and L. Yin, *Nat. Commun.*, 2020, **11**, 5480. For selected examples with aluminium reagents, see: (k) D. Gillingham and A. H. Hoveyda, *Angew. Chem., Int. Ed.*, 2007, **46**, 3860; (l) Y. Lee, K. Akiyama, D. G. Gillingham, M. K. Brown and A. H. Hoveyda, *J. Am. Chem. Soc.*, 2008, **130**, 446.

7 (a) J. Y. W. Mak and C. M. Williams, *Chem. Commun.*, 2012, **48**, 287; (b) F. Meng, K. P. McGrath and A. H. Hoveyda, *Nature*, 2014, **513**, 367; (c) Y. Kanda, H. Nakamura, S. Umemiya, R. K. Puthukanoori, V. R. M. Appala, G. K. Gaddamanugu, B. R. Paraselli and P. S. Baran, *J. Am. Chem. Soc.*, 2020, **142**, 10526.

8 When Grignard reagents are involved, the use of base is not required, see ref. 6c and 6d.

9 S. Drissy-Amraoui, T. E. Schmid, J. Lauberteaux, C. Crévisy, O. Baslé, R. Maria de Figueiredo, S. Halbert, H. Gérard, M. Mauduit and J.-M. Campagne, *Adv. Synth. Catal.*, 2016, **358**, 2519.

10 P. L. Arnold, I. J. Casely, Z. R. Turner and C. D. Carmichael, *Chem.–Eur. J.*, 2008, **14**, 10415.

11 Y.-S. Wong, C. Marazano, D. Gnecco, Y. Génisson, A. Chiaroni and B. C. Das, *J. Org. Chem.*, 1997, **62**, 729.

12 For the intermolecular insertion of alcohols, see for instance: S. Csihony, D. A. Culkin, A. C. Sentman, A. P. Dove, R. M. Waymouth and J. L. Hedrick, *J. Am. Chem. Soc.*, 2005, **127**, 9079.

13 An oxidative/reductive elimination process was recently reported with cyclic(alkyl)(amino)carbenes, see: D. R. Tolentino, S. E. Neale, C. J. Isaac, S. A. Macgregor, M. K. Whittlesey, R. Jazzar and G. Bertrand, *J. Am. Chem. Soc.*, 2019, **141**, 9823.

14 R. Tarrieu, A. Dumas, J. Thongpaen, T. Vives, T. Roisnel, V. Dorcet, C. Crévisy, O. Baslé and M. Mauduit, *J. Org. Chem.*, 2017, **82**, 1880.

15 For selected examples of copper-free AAA, see:(a) Y. Lee and A. H. Hoveyda, *J. Am. Chem. Soc.*, 2006, **128**, 15604; (b) Y. Lee, B. Li and A. H. Hoveyda, *J. Am. Chem. Soc.*, 2009, **131**, 11625; (c) O. Jackowski and A. Alexakis, *Angew. Chem., Int. Ed.*, 2010, **49**, 3346; (d) D. Grassi and A. Alexakis, *Adv. Synth. Catal.*, 2015, **357**, 3171.

16 Any attempt to identify/characterize the active catalytic species involved in the copper-free AAA failed. Nevertheless, based on ref. 15b, we speculated that a Zn(II) hydroxylalkyl-chelating NHC species is formed.

17 For seminal mechanistic insights highlighting the difference between NHC-Cu and the NHC Cu-free catalytic system in AAA, see ref. 15b.

18 Similar Au-complexes were recently found to catalyse efficiently alkoxycyclization of 1,6-enynes: H. F. Jónsson, A. Orthaber and A. Fiksdahl, *Dalton Trans.*, 2021, **50**, 5128.

19 Racemic NHC-alcohol adducts demonstrated efficiency in organocatalytic ring-opening polymerisation of lactide, see ref. 12.